WALAILAK JOURNAL
http://wjst.wu.ac.th Engineering and Physical Sciences

Volatile Organic Compound (VOC) Removal via Photocatalytic Oxidation Using TiO_2 Coated Nanofilms

Sunun KHAMI[1], Wipawee KHAMWICHIT[1,*], Ratthapol RANGKUPAN[2] and Kowit SUWANNAHONG[3]

[1]*School of Engineering and Resources, Walailak University, Nakhon Si Thammarat 80161, Thailand*
[2]*Metallurgy and Materials Science Research Institute, Chulalongkorn University, Bangkok 10330, Thailand*
[3]*Faculty of Public Health, Western University, Bangkok 10510, Thailand*

([*]Corresponding author's e-mail: khamwipawee@gmail.com, kwipawee@wu.ac.th)

Received: 13 October 2016, Revised: 18 June 2017, Accepted: 23 July 2017

Abstract

In this paper, toluene removal via photocatalytic oxidation using TiO_2 dip coated nanofilms is presented. Nanofilms were synthesized from bacterial cellulose using the electrospinning technique. The physical properties of the nanofilms were analyzed by scanning electron microscopy (SEM). The ratio of bacterial cellulose/nylon used in the spinning process was 0.165:1. The results from SEM showed that the structure of the TiO_2 composite nanofilms was rutile crystalline with an average particle size of 20 nm, and synthesized nanofilms had an average size of 20 - 30 nm. The band gap energies of TiO_2-dip coated nanofilms ranged from 3.18 - 3.21 eV. SEM results of TiO_2 coated nanofilms suggested that the TiO_2 was rather uniformly distributed onto the surface of the nanofilms. The actual amount of TiO_2 coated on the nanofilms was estimated using thermogravimetric analysis (TGA) for 1x1 cm^2 surface area. It was found that 0.1852, 0.2897 and 0.7275 mg of TiO_2 were coated on the surface of the nanofilms for 1, 2.5 and 5 % (weight) TiO_2 dosage, respectively. The photocatalytic activity of the nanofilms was tested for the removal of gaseous toluene in a photocatalytic reactor. Experimental conditions were set as follows: UV light intensity of approximately 2.7 $mW.cm^{-2}$, flow rate of 0.2 $L.min^{-1}$, and an initial toluene concentration of about 200±20 ppm, and a retention time at 200 min. The degradation rate of toluene increased with increasing dosage of TiO_2 from 1, 2.5 and 5 %. The nanofilms at a 5 % dosage yielded the highest removal efficiency of 92.71 %, followed by the 2.5 and 1 % dosage, respectively.

Keywords: Photocatalytic oxidation, toluene, nanofilm, volatile organic compound (VOC)

Introduction

Volatile organic compounds (VOCs) are major indoor air pollutants, which are harmful to both human health and the environment. Inhalation of VOCs can cause membrane irritation, breathing difficulties, nausea and damage of the central nervous system as well as other organs. Recently, photocatalytic oxidation (PCO) has received considerable attention as an alternative technology to solve indoor pollution issues [1]. The air purification technique of photocatalytic oxidation commonly uses nano-semiconductor catalysts and ultraviolet (UV) light (300 - 400 nm) to convert organic compounds in indoor air into benign and odorless constituents - water vapor (H_2O) and carbon dioxide (CO_2) [2,3].

Titanium dioxide (TiO_2), the most practical and prevalent photocatalyst used in PCO, has been the target for extensive research due to its various advantages including high reactivity, chemical stability, robustness against photo corrosion, low toxicity and low cost. In addition, it is an environmental friendly process and results in non-toxic final products [4,5]. Several preparation methods used to obtain TiO_2 thin films such as spray coating, spin coating, chemical vapor deposition, have been investigated. Among the

available TiO_2 film preparation methods, the use of nanofilms is one of the effective techniques to synthesize strong membranes. Nanofilms are usually synthesized by petrochemical materials. However, the use of these materials is expensive and causes toxicity to humans and the environment. Therefore, replacing petrochemicals by nanofilms synthesized from agricultural waste is more environmentally friendly. In Thailand, banana trees are easily and widely grown, and banana peels are usually thrown away after banana consumption. A banana peel is mainly composed of cellulose as well as carbon sources for bacteria cellulose production [6].

In the current study, banana-peel bacterial cellulose is produced by *Acetobacter Xylinum*. Nanofilms from the banana-peel bacterial cellulose were synthesized and formed by electrostatic spinning. The films were then dipped into a TiO_2-ethanol solution. The characterization of the nanofilms used scanning electron microscopy (SEM). In addition, the removal efficiency of toluene in the photocatalytic reactor was investigated.

Materials and methods

Bacterial cellulose production

A culture media for banana peels bacterial cellulose production was used (Hestrin & Schramm (HS) medium) with 11 % Brix of sugar concentration for the cultivation. The pH of the medium was initially adjusted to 5.25, and the fermentation medium was sterilized. For cultivation, the cell suspension of *A. xylinum* was inoculated in 100 ml of HS medium in a 500 ml flask. *A. xylinum* dosage to banana peels in DI water of 6.67:1 was prepared. For shaking cultures in a flask, the cell suspension was grown under static conditions at 150 rpm and 30 °C for 5 days [6-11].

Nanofilm sythesis and TiO_2 dip coating on nanofilms as a photocatalyst

Bacteria cellulose was heated at 105 °C for 6 h, then dissolved in 2 mL of formic acid (98 % from Sigma Aldrich). Two grams of nylon (Tm 228.5 °C density 1.084 g/mL at 25 °C) was added into the solution. The solution was spun into nanofilms using electrospinning. The electrospinning process was carried out at a voltage of 20 kV, needle-tip-to-collector distance of 15 cm for 2 h. Nanofilms were dried in a vacuum oven for 24 h [7-11]. Nanoparticle TiO_2 (rutile, 25 nm particle size, 99.7 % from Sigma Aldrich) was dispersed in ethanol to obtain 1, 2.5, and 5 wt%, respectively. Each nanofilm was dipped into the TiO_2 solution at room temperature for roughly 10 min and then put in an oven at 60 °C for 1 h. The dipping process was repeated 3 times. Uncoated-nanofilms and TiO_2-coated nanofilms were characterized by SEM (JxA-840, JEOL, Japan). The actual amount of TiO_2 coating on the surface was estimated by TGA (TGA 4000, Perkin Elmer, USA). The band gap energy of the TiO_2-coated nanofilms was analyzed using a UV-Vis spectrophotometer (Lambda 35, Perkin Elmer, USA) [12,13].

Optical property and band gap energy analysis

Absorbance of ultraviolet-visible spectra of the TiO_2-coated films were analyzed using the UV-VIS spectrophotometer (Lambda 950, Perkin Elmer instrument) equipped with an integrating sphere. All spectra were monitored in the absorbance mode and acquired under ambient conditions. The spectra were measured in the range from 200 to 700 nm. The band gap energy of TiO_2-coated nanofilms was calculated from the absorbance results [1].

VOCs removal of photocatalytic oxidation process

The photocatalytic reactor was set up to study VOCs removal from indoor air using the TiO_2 coated nanofilms as shown in **Figure 1**. Toluene was selected as a representative VOC in the experiments. A batch stainless steel reactor with 700 cm^3 capacity was used in this study. A UV lamp with 300 - 400 nm, having the highest irradiation peak at 395 - 400 nm, was installed in the reactor. The intensity of the ultraviolet light was approximately 520 mW/cm^2. A toluene solution (99.8 %) was injected into the batch reactor to be mixed with air (0.2 L/min) to obtain a 200 ppm toluene concentration at steady state (**Table 1**). Toluene contaminated air was circulated in the system for 20 min, then UV lamp was turned on and the toluene concentration was measured every 10 min. the retention time of experiments was 200 min

[14-18]. Toluene concentrations were measured using a Model Clarus500 GC-MS system (Perkin Elmer). A gas chromatography (GC) column 30 m in length with an inner diameter of 0.25 mm, with helium as a carrier gas (purity 99.99 %), was used for quantification. The injector port temperature was maintained at 150 °C, the oven was programmed with an initial temperature of 30 °C, and then increased, at a rate of 10 °C/min, to 150 °C. Daily calibration curves were prepared with each of the toluene solutions.

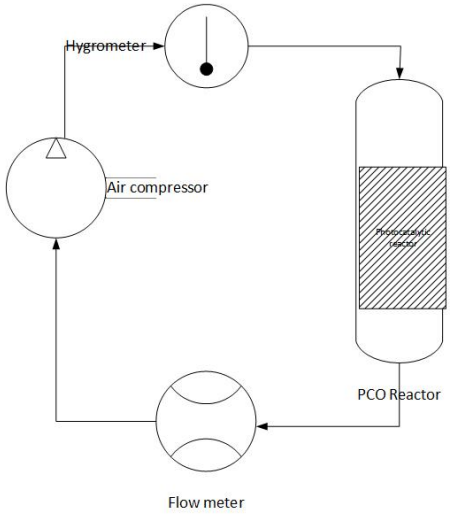

Figure 1 Photocatalytic reactor.

Table 1 Operating conditions for toluene photocatalytic degradation.

Operating conditions	**Representative value**
Initial relative humidity, %	45 - 55 %
Temperature, °C	26 - 50
Air Flow rate, L min^{-1}	0.2
Reactor residence time, min	10
Initial toluene concentration, ppm	200 (±20)
UV light intensity, mW cm^{-2}	530
Reactor material	stainless steel
Dosage of catalyst film, (wt.%. cat/wt. film)	1, 2.5, 5
Reaction time, min	200

Adsorption kinetic or photocatalytic oxidation kinetic

The pseudo-second-order model based on adsorption capacity is shown in Eq. (1) [19];

$$\frac{dq_t}{dt} = k_2 \left(q_e - q_t\right)^2 \quad (1)$$

Integrating Eq. (1) obtains Eq. (2), in which k_2 is the rate constant of pseudo-second order model, q_t is the amount of toluene removal on the surface of the adsorbent at any time (mg/L), t is time (min), and q_e is the amount of toluene removed at equilibrium (mg/L). Integrating Eq. (1) and applying the initial conditions [20], we have;

$$\frac{t}{q_t} = \frac{1}{k_2 q_e^2} + \frac{1}{q_e} t \quad (2)$$

It is noticed that k_2 and q_e in Eq. (2) can be obtained from the intercept and slope in the plot t/q_t vs. t.

Results and discussion

Bacterial cellulose production

Figures 2(a) and **2(b)** illustrate the bacterial cellulose cultivated from *A. xylinum* with banana peels under the conditions described in the previous section and SEM analysis of the bacterial cellulose at 20,000 magnification. From the SEM image, it was found that bacterial cellulose synthesized from banana peels was composed of long fibers with an average diameter around 100 - 120 nm and a length ranging from 100 - 150 nm, which indicated that the synthesized bacterial cellulose was a nanostructure. According to a previous study [21], bacterial cellulose fibers have an average diameter of around 100 nm and a length of 0.5 - 1 μm. **Figure 3** shows the nanofilms obtained from the electrospinning process.

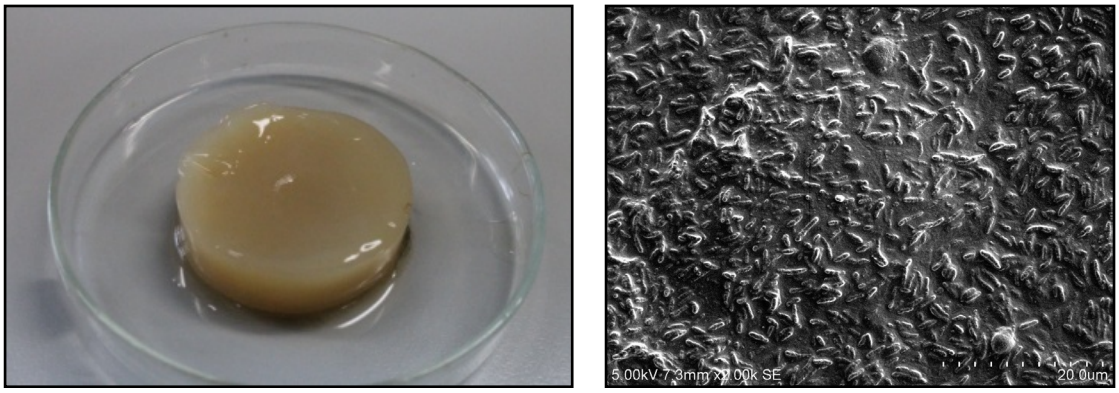

(a) (b)

Figure 2 (a) Bacterial cellulose from banana peels (b) SEM micrograph of bacterial cellulose at 20,000×.

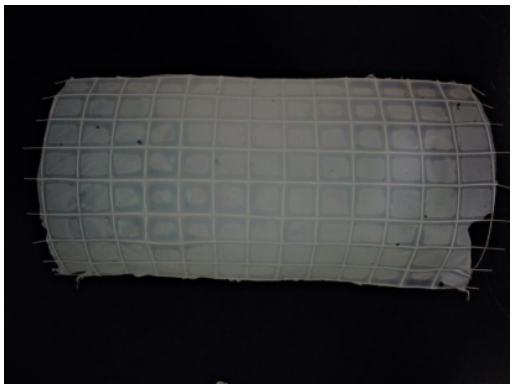

Figure 3 Nanofilm from bacterial cellulose of banana peels.

Characterization of nanofilms and TiO_2 dip coated nanofilms

Figure 4 displays the TiO_2-dip coated nanofilms and SEM analysis for different dosages of TiO_2. As seen in the figure, each nanofilm synthesized in the study was approximately 20 - 30 nm in size. Distribution of TiO_2 appeared to be mostly on the surface of the nanofilms. Uniform distribution could be observed for higher dosages of TiO_2. The nanofilm thickness was estimated through thickness measurements of thin film using a Benetech model GM210. The average film thickness found in this study was 0.13 mm.

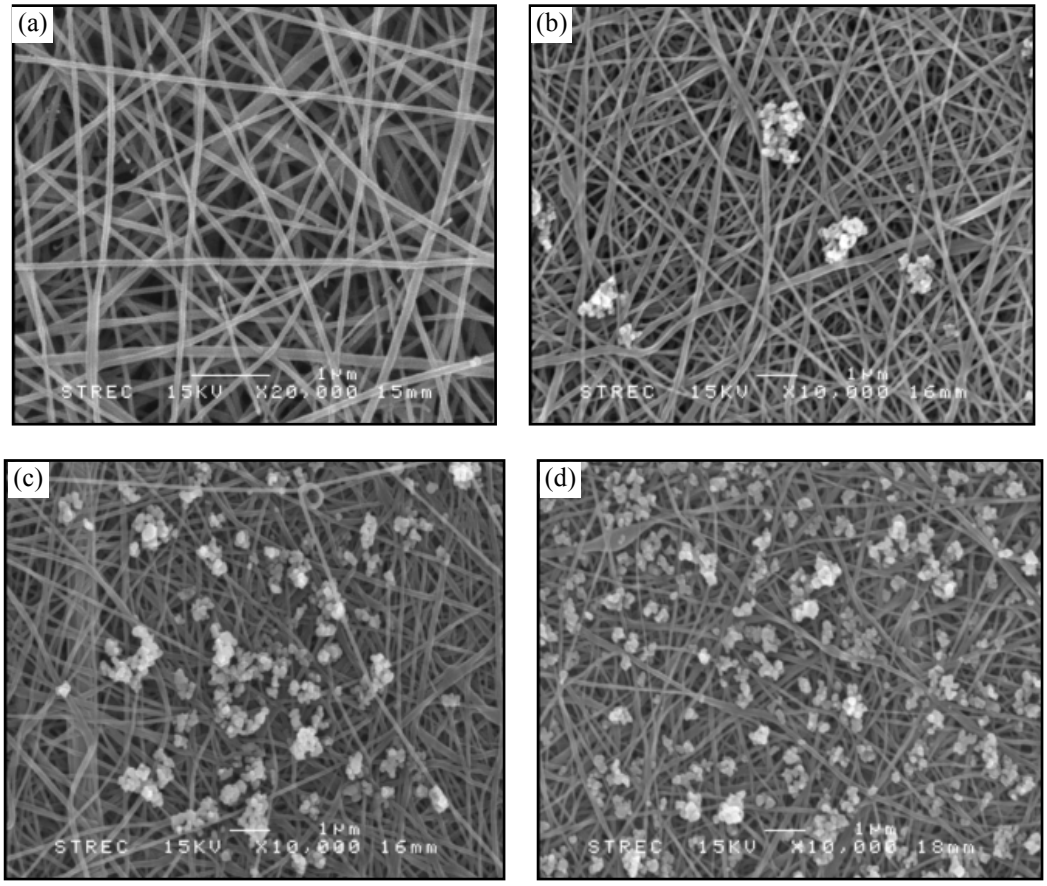

Figure 4 SEM micrograph of (a) Nanofilm, (b) Dip coating TiO_2 1% , (c) Dip coating TiO_2 2.5 % and (d) Dip coating TiO_2 5 %.

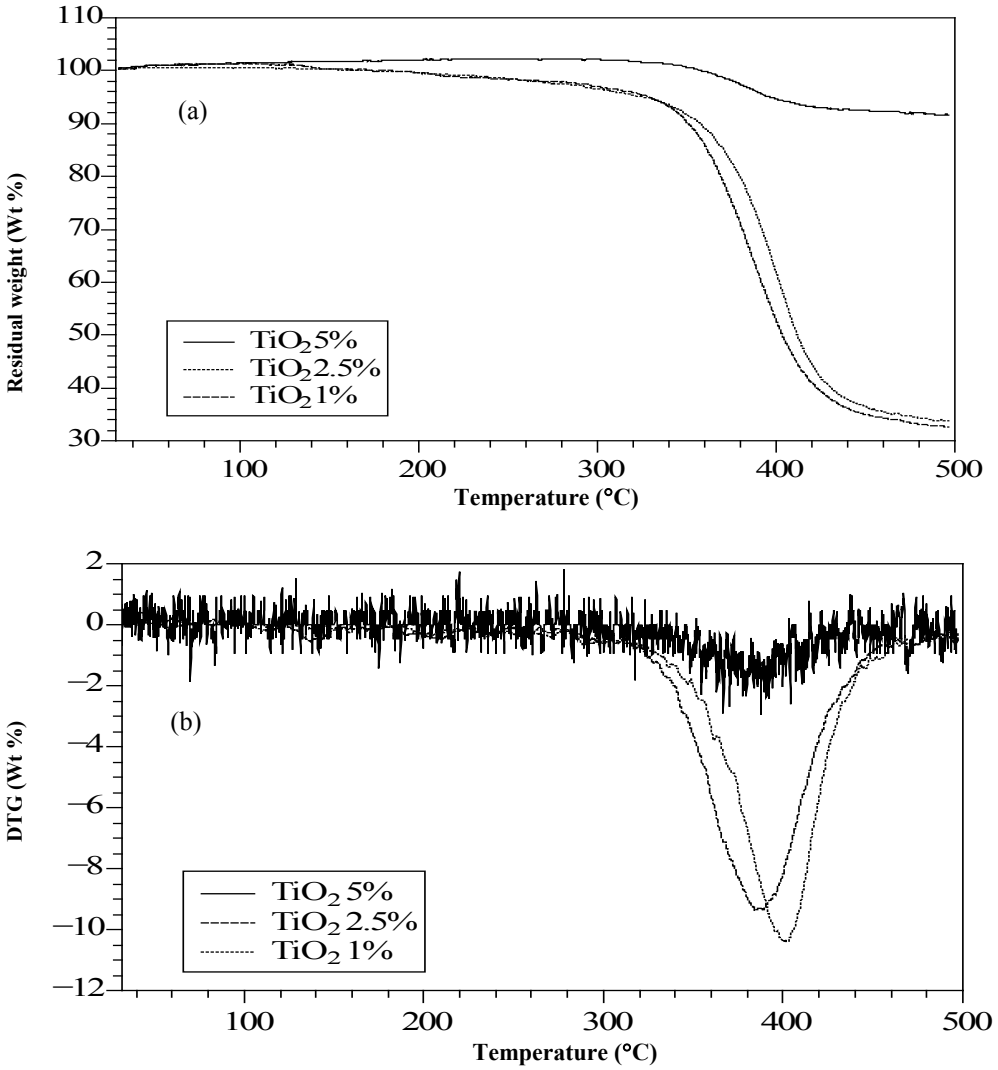

Figure 5 (a) TGA thermograms in nitrogen atmosphere at a heating rate of 20 °C/min and (b) DTG thermograms in nitrogen atmosphere at a heating rate of 20 °C/min.

TG and DTG thermograms at a heating rate of 20 °C /min from room temperature to 500 °C are shown in **Figures 5(a)** and **5(b)**. The thermal decomposition process of all the samples can be divided into 2 distinguishable stages. The first stage, ranged from room temperature to approximately 300 °C, was a result of moisture evaporation and possible degradation of light organic compounds. The second stage, ranged from approximately 300 to 500 °C, was the main devolatilization process, during which intense decomposition of bacterial cellulose and nylon in the samples was observed. The carbonization process inducing weight loss due to nylon and bacterial cellulose evaporization occurred in this stage. Similar results can also be observed from the TGA and DTG thermograms in nitrogen atmosphere at a heating rate of 20 °C /min (**Figure 5(b)**). The majority of weight loss was according to condensation of hydroxyl groups at the particle surface in the range of 300 - 500 °C [12,22,23]. As seen in **Figures 5(a)** and **5(b)**, the 5 % TiO_2-coated onto nanofilms was higher than that of 2.5 and 1 % TiO_2-coated nanofilms. These percent weights correspond to the amount of TiO_2 coated on the nanofilms. DTG (Wt%) results indicated

that higher dosages of TiO_2 affect the thermal stability of the coated nanofilm. **Table 2** shows percentages of mass change after thermal decomposition by TGA for 1, 2.5 and 5% TiO_2-coated nanofilms. The mass change for the 5 % TiO_2-coated nanofilms was smallest, followed by 2.5 and 1 % TiO_2-coated, respectively. This calculation was estimated using the final weight (%) from TGA results.

Table 2 Mass Change (%) of TiO_2-coated nanofilm.

No.	Sample Mass (mg)	Mass at final time (%)	Mass at final time (mg)	Mass Change (%)
$TiO_2$1%	0.569	32.530	0.1852	67.47
$TiO_2$2.5%	0.860	33.690	0.2897	66.31
$TiO_2$5%	0.794	91.624	0.7275	8.38

Band gap energy of TiO_2

UV absorbance spectra of the nanofilm at various amounts of nano-TiO_2 are shown in **Table 3**. As seen in **Table 3**, the commercial TiO_2 absorbed UV light at 400 nm, while the 1, 2.5 and 5 wt% nano-TiO_2 coated nanofilms absorbed UV light at 396, 397 and 399 nm, respectively. As seen in the last column of **Table 3**, the difference in band gap energy (E) of TiO_2 coated nanofilm compared with that of commercial TiO_2 was very small and negligible. Thus, the bacterial cellulose nanofilms did not affect the band gap energy of TiO_2.

Table 3 Band gap energy of the nanofilm at various amounts of TiO_2.

Code	λ (nm)	E (eV)	% difference of E(eV) from commercial TiO_2
Commercial TiO_2	400	3.22E-01	0.0000
$TiO_2$1%	395	3.18E-01	0.0126
$TiO_2$2.5%	397	3.20E-01	0.0062
$TiO_2$5%	399	3.21E-01	0.0031

Toluene removal by photocatalytic oxidation process

The photocatalytic oxidation system set up as described in the previous section was utilized to study the toluene removal from indoor air. TiO_2-coated nanofilms with 3 different dosages of TiO_2 were used in the photocatalytic reactor. The initial concentration of toluene in the system was approximately 200 ppm. Toluene removal efficiency is displayed in **Figure 6**. As seen in **Figure 6**, the percentage removal of toluene increased as the amount of TiO_2 coated onto the film increased. However, when the amount of TiO_2 was increased from 2.5 to 5 %, a significant difference in removal could not be observed. These results were in agreement with the previous work [2].

The possible explanation drawn from these results was that the higher dosage of TiO_2 deposited on the surface enhanced a larger active surface site apart from nucleation of TiO_2 particles on the nanofilm substrate. Consequently, a higher toluene removal was obtained for higher TiO_2 dosage. The percentage removal of toluene by TiO_2 coated nanofilms was calculated using the following equation;

$$\%Removal = \left(\frac{C_0 - C_e}{C_0} \right) \times 100 \quad (3)$$

where C_0 is the initial concentration of toluene and C_e is the equilibrium concentration.

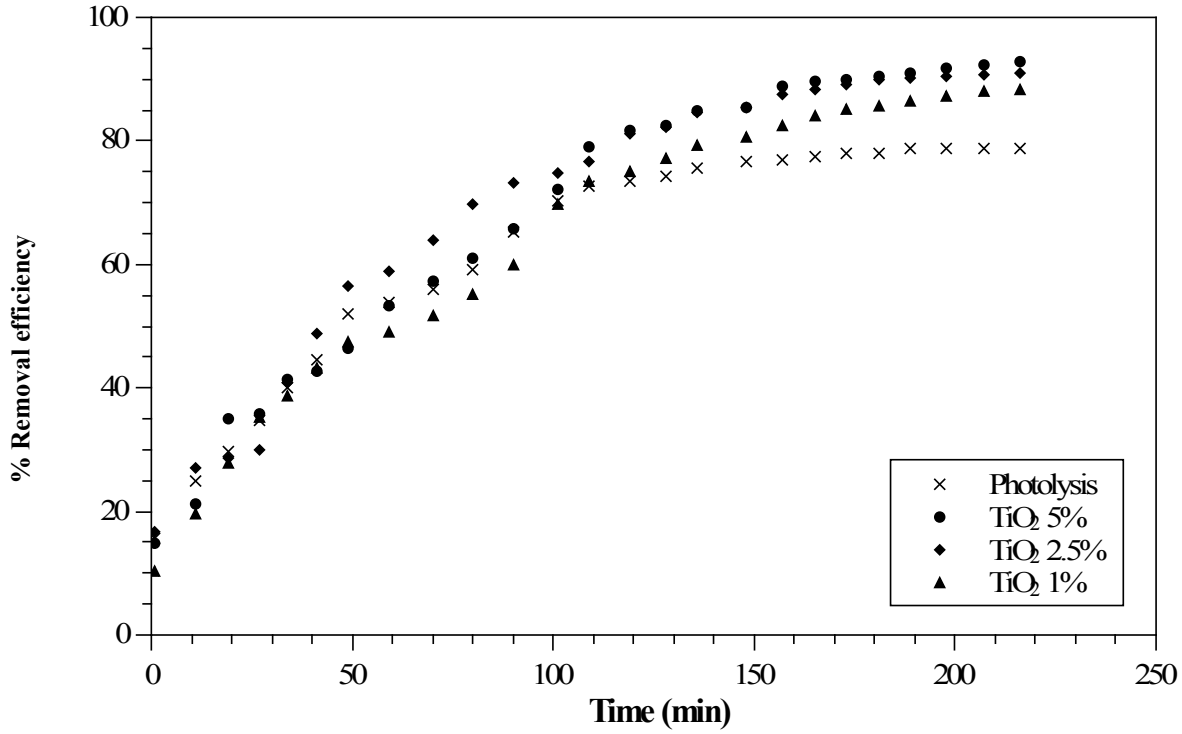

Figure 6 Toluene removal by photocatalytic oxidation process.

Adsorption kinetic or Photocatalytic oxidation kinetic

The pseudo-second-order model Eq. (2) gave the best fitting to describe the toluene adsorption mechanism onto nanofilms in the reactor (R^2 = 0.996), as shown in **Figure 7**. The pseudo-second order mechanism has been widely used for the explanation of catalytic oxidation of VOCs over metal oxides, which involves the reaction between VOC molecules and oxygen on different redox sites of the catalyst surface [24,25].

In this study, the pseudo-second-order mechanism was presumed as the mechanism for toluene oxidation. **Figure 7** displays t/q_t vs time for 4 different cases. The first case was photolysis (i.e., 0% TiO_2-coated), the rest were 1, 2.5 and 5 % TiO_2-coated nanofilms. All the curves in **Figure 7** were obtained using the pseudo-second-order mechanism as described in the method section. Linear regression, R^2, of all cases were closed to 1.0 (0.996, 0.992, 0.994, 0.989), thus it suggests that the pseudo-second-order mechanism is dominant in toluene removal.

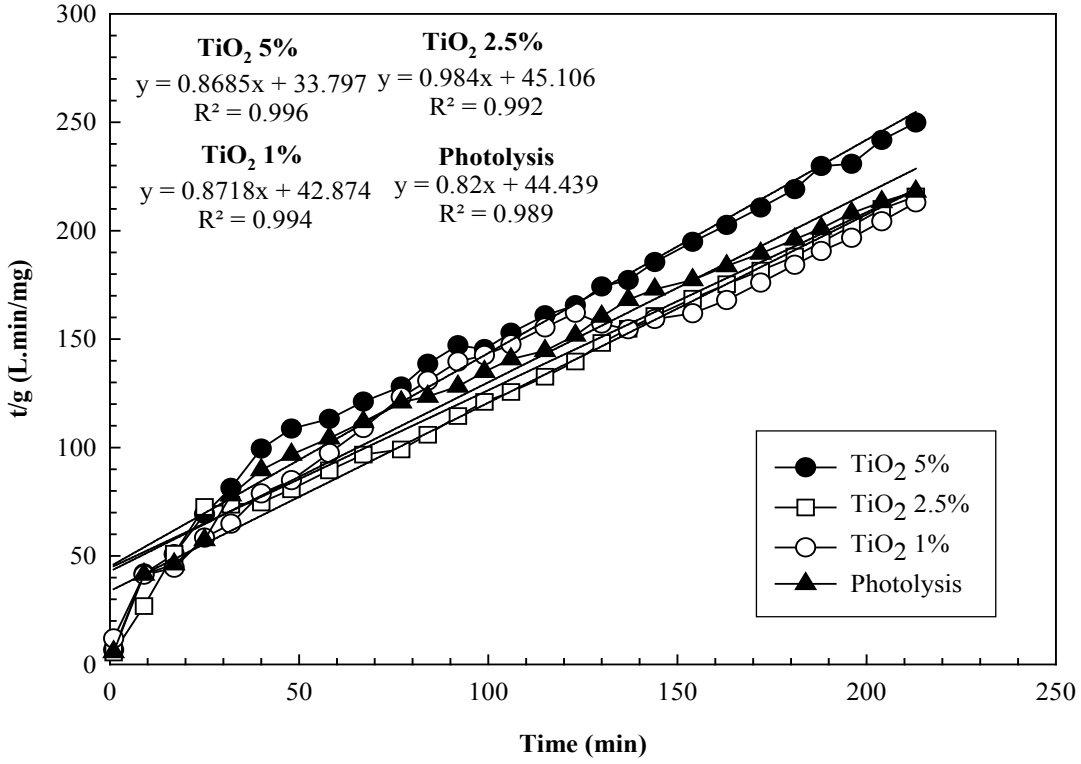

Figure 7 Conversion of toluene: pseudo-second-order model.

Conclusions

TiO_2-coated nanofilms synthesized from banana peels using the electrospinning method can potentially be used in photocatalytic reactors to remove toluene contaminated air. According to the experimental results, the higher dosage of TiO_2 coating yielded a higher removal efficiency. Since agricultural waste was used in the synthesis of these nanofilms, this study also offers a potential means of environmental conservation and waste minimization for indoor air treatment processes.

Acknowledgements

This work was supported by the Walailak University Fund and Walailak University Grant No. WU58610.

References

[1] K Suwannahong, S Sinvithayapakorn, P Noophan and W Sanongraj. Improvement of TiO_2/LDPE composite films for photocatalytic oxidation of acetone. *Adv. Mater. Res*. 2014; **931**, 235-40.
[2] K Suwannahong, W Sanongra, J Kruenate, S Phibanchon, S Jawjit and W Khamwichit. Photo catalytic oxidation degradation of volatile organic compound with nano-TiO_2/LDPE composite film. *Int. J. Chem. Mole. Nec. Mate. Meta. Eng*. 2013; **7**, 1.
[3] K Suwannahong, W Liengcharernsit, W Sanongraj and J Kruenate. Application of Nano-TiO_2 /LDPE composite film on photocatalytic oxidation degradation of dichloromethane. *J. Environ. Bio.* 2012; **33**, 955-9.
[4] ML Bechec, N Kinadjianb, OR Backov and S Lacombea. Comparison of kinetics of acetone, heptane and toluene photocatalytic mineralization over TiO_2 microfibers and Quartzel mats. *Appl. Catal. B: Environ.* 2015; **179**, 78-87.
[5] W William, AJ Daniel, MB John, AF James, EB Leann, MV Marya and CG Suzanne. Heterogeneous photocatalysis for control of volatile organic compounds in indoor air. *J. Air Waste Manag. Assoc.* 1996; **46**, 891-8.
[6] S Khami, W Khamwichit, K Suwannahong and W Sanongraj. Characteristics of bacterial cellulose production from agricultural wastes. *Adv. Mater. Res*. 2014; **931-932**, 693-7.
[7] M Mehrab, A William, M Murray and M Park. Non-linear parameter estimation for a dynamic model in photocatalytic reaction. *Chem. Eng. Sci*. 2000; **55**, 4885-91.
[8] C Mendozaa, A Vallea, M Castellote, A Bahamondea and M Faraldos. TiO_2 and TiO_2-SiO_2 coated cement: Comparison of mechanic and photocatalytic properties. *Appl. Catal. B: Environ.* 2015; **178**, 155-64.
[9] M Aihong, C Shen, Z Hui, L Yanqiu, Z Yanguo and L Qinghai. Pyrolysis and simulation of typical components in wastes with macro-TG. *Fuel* 2015; **157**, 1-8.
[10] SO Han, JH Youk, KD Min, YO Kang and WH Park. Electrospinning of cellulose acetate nanofibers using a mixed solvent of acetic acid/water: Effects of solvent composition on the fiber diameter. *J. Mater. Lett.* 2008; **62**, 759-62.
[11] KC Seavey and WG Glasser. Continuous cellulose fiber reinforced cellulose ester composites. II. Fiber surface modification and consolidation conditions. *J. Cellulose* 2001; **8**, 161-9.
[12] S Pazokifard, S Farrokhpay, M Mirabedini and M Esfandeh. Comparative Study on sol-gel treatment of TiO_2 nanoparticles using different fluorosilane-based compounds. *Eng. Aust*. 2013; **41**, 26-31.
[13] M Ou, F Dong, W Zhang and Z Wu. Efficient visible light photocatalytic oxidation of NO in air with band-gap tailored $(BiO)_2CO_3$–BiOI solid solutions. *Chem. Eng. J*. 2014; **255**, 650-8.
[14] SW Yao and HP Kuo. Photocatalytic degradation of toluene on SiO_2/TiO_2 photocatalyst in a fluidized bed reactor. *Proc. Eng.* 2015; **102**, 1254-60.
[15] C Guillard, D Debayle, A Gagnaire, H Jaffrezic and JM Herrmann. Physical properties and photocatalytic efficiencies of TiO_2 films prepared by PECVD and sol-gel methods. *Mat. Res. Bullet.* 2004; **39**, 1445-58.
[16] J Kasanen, J Salstela, M Suvanto and TT Pakkanen. Photocatalytic degradation of methylene blue in water solution by multilayer TiO_2 coating on HDPE. *Appl. Surf. Sci.* 2011; **258**, 1738-43.
[17] DF Ollis. Photocatalytic purification and remediation of contaminated air and water. *J. Chem.* 2000; **3**, 405-11.
[18] S Singh, H Mahalingam and PK Singh. Polymer-supported titanium dioxide photocatalysts for environmental remediation: A review. *Appl. Catal. A Gen.* 2013; **462-463**, 178-95.
[19] FC Wua, RL Tseng, SC Huang and RS Juang. Characteristics of pseudo-second-order kinetic model for liquid-phase adsorption: A mini-review. *Chem. Eng. J.* 2009; **151**, 1-9.
[20] S Khami, W Khamwichit and C Siripatana. Kinetic and linear equation of adsorption by Tio_2 nanofilm coating in photocatalytic reactor. *J. Eng. Appl. Sci.* 2016; **11**, 2490-4.
[21] D Onggo, OK Putri and M Aminah. Utilization of nata de coco as a matrix for preparation of thin film containing spin crossover iron (II) complexes. *Mater. Sci. Eng*. 2015; **79**, 1-5.

[22] A Zheng, Z Zhao, S Chang, Z Huang, F He and H Li. Effect of torrefaction temperature on product distribution from two-staged pyrolysis of biomass. *Energ. Fuels* 2012; **26**, 2968-74.
[23] TS Radoman, JV Dunuzovi, KT Trifkovi, T Palija, AD Marinkovi, B Bugarski and ES Dunuzovi. Effect of surface modified TiO_2 nanoparticles on thermal, barrier and mechanical properties of long oil alkyd resin-based coatings. *Express Polym. Lett*. 2015; **9**, 916-31.
[24] JJ Pei, and JSS Zhang. Critical review of catalytic oxidization and chemisorption methods for indoor formaldehyde removal. *HVAC&R Res*. 2011; **17**, 476-503.
[25] X Liang, Q Feihong, P Liu, G Wei, S Xiaoli, M Lingya, H Hongping, X Lin, Y Xi, J Zhu and R Zhu. Performance of Ti-pillared montmorillonite supported Fe catalysts for toluene oxidation: The effect of Fe on catalytic activity. *Appl. Clay Sci.* 2016; **132-133**, 96-104.